

THE EFFECT OF THERMO-MECHANICAL PROCESSING ON THE MECHANICAL PROPERTIES
OF MOLYBDENUM - 2 VOLUME % LANTHANA

A.J. Mueller - Bechtel Bettis Inc.
J.A. Shields, Jr. - CSM Industries Inc.
R.W. Buckman, Jr. - Refractory Metals Technology

DE-AC11-98PN38206

NOTICE

This report was prepared as an account of work sponsored by the United States Government. Neither the United States, nor the United States Department of Energy, nor any of their employees, nor any of their contractors, subcontractors, or their employees, makes any warranty, express or implied, or assumes any legal liability or responsibility for the accuracy, completeness or usefulness of any information, apparatus, product or process disclosed, or represents that its use would not infringe privately owned rights.

BETTIS ATOMIC POWER LABORATORY

WEST MIFFLIN, PENNSYLVANIA 15122-0079

Operated for the U.S. Department of Energy
by Bechtel Bettis, Inc.

Abstract

Variations in oxide species and consolidation method have been shown to have a significant effect on the mechanical properties of oxide dispersion strengthened (ODS) molybdenum material. The mechanical behavior of molybdenum - 2 volume % La_2O_3 mill product forms, produced by CSM Industries by a wet doping process, were characterized over the temperature range of -150°C to 1800°C . The various mill product forms evaluated ranged from thin sheet stock to bar stock. Tensile properties of the material in the various product forms were not significantly affected by the vast difference in total cold work. Creep properties, however, were sensitive to the total amount of cold work as well as the starting microstructure. Stress-relieved material had superior creep rupture properties to recrystallized material at 1200°C , while at 1500°C and above the opposite was observed. Thus it is necessary to match the appropriate thermo-mechanical processing and microstructure of molybdenum - 2 volume % La_2O_3 to the demands of the application being considered.

Introduction

Historical Background: Very fine dispersed second phases have long been recognized as a way to improve the elevated-temperature strength of metals and alloys (1,2). The basic theoretical background established several criteria for success, directed primarily at insuring strong particle-dislocation interactions and thus high hardening rates at low temperatures. These criteria included (1):

- Small interparticle spacing.
- High hardness of the dispersed phase.
- Low matrix-particle interfacial energy.

For the dispersant to provide effective creep resistance, additional criteria were identified, including (1):

- High free energy of formation for the dispersed phase particles to enhance particle stability.
- A low or negligible solubility for components of the dispersed phase in the matrix.
- Low diffusivity of the components of the dispersed phase in the matrix.

Attempts in the fifties to attain these goals were not particularly successful (3), although several different matrix-particle systems were investigated. In these early cases, the materials under investigation suffered from particle sizes that were simply too large to have the desired beneficial effect.

One refractory metal alloy class stood out during this time as a highly creep-resistant material, namely AKS-doped tungsten (4,5). It had been long known that tungsten when doped in very specific ways with very small amounts of oxides of aluminum, potassium, and silicon, displayed extraordinary resistance to creep after recrystallization. This creep resistance was connected to the unique elongated grain structure that evolved during recrystallization. A full understanding of this effect was not gained until the seventies, when the work of several investigators (6,7) identified the operative mechanism in the alloy system. They showed that the doping produced a very fine array of potassium bubbles, which were highly deformed by the wire drawing process used for making lamp filament wire. The thermal energy applied to recrystallize the tungsten also caused these "tubes" to break into linear arrays of submicron equiaxed bubbles. The bubble arrays provided strong barriers to grain growth perpendicular to their length, but little resistance along the length, providing a highly elongated creep-resistant recrystallized grain structure.

This understanding also prompted efforts to manufacture oxide-dispersed materials, and in the same era great progress was made in manufacturing analogues of AKS-doped tungsten using oxide particles in both tungsten (8) and nickel (9,10). The fundamental criteria were shown to be independent of material system, and essentially the same or very similar to those identified in the early theoretical work on dispersion hardening.

A variety of approaches have been pursued to produce fine, stable oxide dispersoids in molybdenum (11-13). The literature hints that materials were made that satisfied the creep resistance criteria (14,15), following the model of thoriated tungsten. However, no creep test data were reported for these materials. In the late eighties, success was demonstrated using rare earth oxides to produce the dispersoids (16). Again it was shown that if fine dispersoids are produced and the material is highly worked before recrystallization, a highly creep-resistant material resulted.

Doping Techniques and Oxide Species: Our previous investigations into the choice of doping technique and oxide species (17) were used to guide the system and doping technique used in this work. Figure 1 illustrates the effect of doping technique and species on tensile properties of ODS molybdenum-lanthana and ODS molybdenum-yttria alloys. The figure legend notes the average oxide particle size obtained in the wrought product using both wet and dry doping techniques. For both oxide species, the wet doping technique results in a much finer dispersion of oxide. At ambient temperatures the alloy's strength is not strongly sensitive to either doping technique, but at high temperatures the wet doping technique produces superior material for a given oxide species. Lanthana-doped material is also superior to Yttria-doped material at elevated temperature.

The superiority of the lanthana-doped material is clearly shown in Figure 2, which is a summary of creep test results obtained from a variety of molybdenum-base materials. In addition to the lanthana- and yttria-doped materials shown in Figure 1, the creep behavior of arc-cast molybdenum (18) and Z6, a commercial zirconia-doped material, are shown. The superiority of the wet-doped molybdenum-lanthana is apparent.

The work reported here focuses on molybdenum doped with lanthanum oxide (La_2O_3), using the wet doping process developed by Bianco, et. al. (19). This approach employs an aqueous lanthanum nitrate solution to dope the molybdenum dioxide (MoO_2) precursor before its reduction to molybdenum metal powder. The process achieves a very fine dispersion of the La_2O_3 in the metal powder, which imparts excellent high-temperature properties. The experimental work reported in this paper was designed to evaluate the efficacy of the Bianco/Buckman doping technique by characterizing the high-temperature properties of pilot- and production-scale heats of ODS molybdenum in both round and flat product forms.

Material Description

The starting material that was used to produce the various mill forms for mechanical property evaluation was produced by CSM Industries by the patented wet doping process that has been described previously (19). The ODS molybdenum material contained nominally two volume percent La_2O_3 that corresponds to a lanthanum (La) analyzed content of 1.09 weight percent. Various consolidation methods and thermo-mechanical working schedules were used to produce the mill forms evaluated. The total amount of work in the final product forms varied from 92% to 99.6% work which represents a reduction in area ranging from 12/1 to 200/1. Flat sheet was produced by cold isostatic pressing (CIP) a rectangular sheet bar which was subsequently sintered and rolled to final gage starting at elevated temperatures and finishing at near room temperature. The 0.188 inch (4.8mm) diameter round bar was processed from a 2.75 inch (70mm) diameter CIP'ed billet which was sintered, and then processed to final form by a combination of rod rolling and swaging at elevated temperature. The 1.5 inch (38mm) diameter bar was consolidated by CIP'ing a nominal 11 inch

(280mm) diameter billet which was sintered and then extruded hot to sheet bar at a 4/1 reduction. A section of the sheet bar was then turned to a 2.75 inch (70mm) diameter round and then rod rolled to final diameter. The final as-worked microstructure was typical for an as-worked material. After a high temperature (>1600°C) annealing treatment, a highly elongated interlocking grain microstructure, typical for an oxide dispersion strengthened material developed (20).

Experimental Procedures

Tensile and creep rupture specimens were machined from the various final product forms. All specimens were pickled to remove 0.001-0.002 inches (25 - 50 μm) from each of the as-machined surfaces in the gage section. Additionally, low temperature tensile specimens were electropolished in a room temperature solution, containing four parts concentrated reagent grade sulfuric acid and one part distilled and/or deionized water, using a 0.010 inch (0.25 mm) thick Type 304 stainless steel cathode and a direct current accelerating potential of 6 - 7 volts to remove 0.001-0.002 inches (25 - 50 μm) from the gauge section.

Mechanical Properties: The following mechanical properties were measured for the ODS molybdenum: (a) 0.2% offset yield stress, (b) ultimate tensile stress, (c) percent reduction in area, and (d) total elongation to failure. The ductile-to-brittle transition temperature (DBTT) was measured by uniaxially loading tensile specimens to failure at temperatures ranging from +200 to -196°C (+392 to -321°F) per ASTM Standards E8 and E21 and a strain rate of 0.05 min^{-1} or 0.00083 sec^{-1} . The surface of each fractured tensile specimen was analyzed with a scanning electron microscope (SEM) to identify the mode of fracture; i.e., ductile or dimpled, cleavage, intergranular, or mixed-mode. The DBTT was defined as the lowest test temperature at which 100% dimpled fracture surfaces were observed, i.e. no cleavage type failure. The elevated temperature tensile properties of the swaged and recrystallized condition were measured by uniaxially loading a tensile specimen to failure in dynamic vacuum (< 5×10^{-5} Torr) at temperatures ranging from 1000 to 1800°C (1832 to 3272°F) and a strain rate of 0.05 min^{-1} or 0.00083 sec^{-1} .

The uniaxial creep-rupture behavior of the ODS molybdenum material was evaluated at temperatures in the range of 1200 to 1800°C (2192 to 3272°F) under ultra-high vacuum (UHV) conditions (< 1×10^{-7} Torr) using internally dead weight loaded machines as described by Buckman and Hetherington (21). The entire system including the test specimen was sealed, baked-out for fourteen hours under dynamic vacuum at 225°C (437°F) to remove all adsorbed moisture and gases from all internal surfaces. The system including the test specimen was heated to the desired test temperature and held for thirty minutes with no load on the specimen. Length change of the gage section was monitored with an optical extensometer with a resolution of 50 micro-inches (1.25 μm). Measurements were made using the shoulders of the gauge section for reference. The first length measurement was made with no load on the specimen, and the first length change measurement was made immediately after the load was applied. Length change measurements were taken at periodic intervals to define the creep deformation behavior of the specimen.

Results and Discussion

Tensile Properties: The longitudinal tensile properties of the ODS molybdenum lots in the as-worked and stress relieved condition are shown in Figure 3. The percent cold work (work at temperatures lower than the recrystallization temperature) is noted for each in the legend. From the yield strength behavior, one can see that the differences in the amount of cold work have a limited effect on the ambient temperature (< 300°C) strength but almost no effect on the elevated temperature strength of the ODS molybdenum material. The ambient temperature ductility is affected by the total amount of cold work to some extent as well. The lots that were worked to a lesser degree (1.5 inch / 38mm

diameter bar and 0.25 inch / 6.3mm thick sheet) have higher room temperature elongation. Also evident from the elongation plot is that the DBTT for all the lots is well below room temperature. The observed DBTT values are listed in Table 1. Scanning electron microscopic evaluations of the fracture appearance confirmed fully ductile transgranular shear below room temperature consistent with previously reported fractography (20).

Creep-Rupture Properties: Unlike the short-time tensile strength, the creep properties are significantly affected by the total amount of cold work. Figure 4 shows the UHV creep behavior of the 1.5 inch (38 mm) diameter bar and 0.188 inch (4.8 mm) diameter rod along with another developmental lot of recrystallized ODS molybdenum rod at 1600°C (2912°F) and 5 ksi (34.5 MPa). As shown in this figure, the total work dramatically affects the degree of primary strain exhibited but has little if any affect on the steady state creep rate. This plot also points out the danger of reporting only minimum creep rate for use as the comparison between materials or differences in thermo-mechanical processing of a single material.

Metallurgical Condition: In addition to the total amount of cold work, the final end use temperature for ODS molybdenum needs to be considered in choosing the appropriate microstructure for optimum creep resistance. A comparison of creep rupture life of ODS molybdenum as a function of metallurgical condition and test temperature is shown in Table 2 compared to unalloyed molybdenum (18). As is indicated from this table, at all temperatures, ODS molybdenum is vastly superior to unalloyed molybdenum. At the lower test temperature (1200°C) ODS molybdenum in the stress relieved condition has over three times the creep rupture life as the same material tested in the recrystallized condition. At higher temperatures (1500°C and 1700°C) the opposite result is observed, the recrystallized material had exceeded three times the rupture life of the stress relieved ODS molybdenum.

Conclusions

The wet doping process in combination with a selected oxide species produced oxide dispersion strengthened (ODS) molybdenum with a combination of high temperature creep rupture strength and a ductile-to-brittle transition temperature (DBTT) well below room temperature. The thermo-mechanical working schedule which ranged from an area reduction of 12/1 to over 200/1 had limited effect on the tensile properties over the temperature range of -100 to 1800°C (-148 to 3272°F). However, the thermo-mechanical working schedule did have a large impact on high temperature creep rupture strength. The processing schedule and final metallurgical condition must be tailored to fit the final application. At temperatures near or less than $0.5T_m$ (1172°C / 2142°F), the stress-relieved microstructure provided the optimum creep rupture strength. The opposite was observed at temperatures much greater than $0.5T_m$ where the recrystallized microstructure provided the highest creep rupture strength.

References

1. R.F. Bunshah and C.G. Goetzel, "A Survey of Dispersion Strengthening of Metals and Alloys," WADC-TR-59-414 Wright Air Development Division, Air Research and Development Command, USAF (July, 1959).
2. B.A. Wilcox, "Basic Strengthening Mechanisms in Refractory Metals," in Refractory Metals and Alloys: Metallurgy and Technology, I. Machlin, R.T. Begley, and E.D. Weisert, Eds., Plenum Press, New York, pp 1-39 (1968).

3. W.L. Bruckart and R.I. Jaffee, "High-Temperature Properties of Molybdenum-Rich Alloy Compositions Made by Powder Metallurgy Methods," Symposium on Metallic Materials for Service at Temperatures Above 1600 F, ASTM STP 174, American Society for Testing Materials, Philadelphia, pp 111-134 (1955).
4. W.D. Coolidge, "Tungsten and Method of Making the Same for Use as Filaments of Incandescent Lamps and for Other Purposes," US Patent 1,082,933 (1913).
5. A. Pacz, "Metal and Its Manufacture," US Patent 1,410,499 (1922).
6. D.M. Moon and R.C. Koo, "Mechanism and Kinetics of Bubble Formation in Doped Tungsten," Met. Trans. 2, pp 2115 (1971).
7. H.G. Sell, D.F. Stein, R. Stickler, A. Joshi, and E. Berkey, "The Identification of Bubble-Forming Impurities in Doped Tungsten," J. Inst. of Metals 100, pp 275 (1972).
8. G.W. King and H.G. Sell, "The Effect of Thoria on the Elevated-Temperature Tensile Properties of Recrystallized High-Purity Tungsten," Trans. Met. Soc. AIME 33, pp 1104-1113 (1965).
9. B.A. Wilcox and A.H. Clauer, "High-Temperature Creep of Ni-ThO₂ Alloys," Oxide Dispersion Strengthening, Proc. Second Bolton Landing Conference, Gordon & Breach, New York pp 323 (1967).
10. J.J. Petrovic and L.J. Ebert, "Elevated Temperature Deformation of TD-Nickel," Met. Trans. 4, pp 1301-1308 (1973).
11. N.J. Grant, "Dispersion Strengthening of Metals and Alloys," US Patent 3,434,830 (1969).
12. C.E.D. Rowe and G.R. Hinch, "Sintered Molybdenum Alloy Process," US Patent 4,622,068 (1986).
13. S. Härdtle and R. Schmidberger, "Wolfram und Molybdän mit Oxiddispersion, Herstellung und Eigenschaften," Proc. 12th International Plansee Seminar '89, Vol. 1, H. Bildstein and H.M. Ortner, Eds., Metallwerk Plansee, Reutte, pp 53-64 (1989).
14. J.E. White, "Alloy and Dispersion Strengthening by Powder Metallurgy," J. Metals, pp 587-593 (1965).
15. J.E. White and R.Q. Barr, "Dispersion-Strengthened Molybdenum and Molybdenum-base Alloys," TDR-669(6250-10)-1 (1965).
16. M. Endo, K. Kimura, T. Udagawa, S. Tanabe, and H. Seto, "The Effects of Doping Molybdenum Wire with Rare Earth Elements," Proc. 12th International Plansee Seminar Vol. 1, H. Bildstein and H.M. Ortner, Eds., Metallwerk Plansee, Reutte, pp 37-52 (1989).
17. R. Bianco and R.W. Buckman, Jr., "Evaluation of Oxide Dispersion Strengthened (ODS) Molybdenum Alloys," Presented at 1995 Spring ASM/TMS Symposium on High Temperature Materials, May 19, 1995, GE CR&D Center, Schenectady, NY (WAPD-T-3073).
18. J.B. Conway and P.N. Flagella, Creep-Rupture Data for the Refractory Metals to High Temperatures, Gordon & Breach Science Publishers, New York (1971).

19. R. Bianco, R.W. Buckman, Jr., and C.B. Geller, "High Strength, Creep-Resistant Molybdenum Alloy and Process For Producing the Same," US Patent 5,868,876 (1999).
20. R. Bianco and R.W. Buckman, Jr., "Mechanical Properties of Oxide Dispersion Strengthened (ODS) Molybdenum," Molybdenum and Molybdenum Alloys, A. Crowson, E. S. Chen, J. A. Shields, and P. R. Subramanian, Eds., The Minerals, Metals & Materials Society, 125-142 (1998).
21. R.W. Buckman, Jr. and J. S. Hetherington, "An Apparatus for Determining Creep Behavior Under Conditions of Ultra High Vacuum," Rev. Sci. Instr., 37, 999-1003 (1966).

Table 1. Ductile-to-brittle transition temperature (DBTT) of stress relieved ODS molybdenum and unalloyed molybdenum.

Material/Form	Size	DBTT (°C)
P/M Mo rod	0.188 inch (4.8 mm) dia.	< -25
ODS Mo rod	0.188 inch (4.8 mm) dia.	< -100
ODS Mo bar	1.5 inch (38 mm) dia.	< -100
ODS Mo sheet	0.030 inch (0.75 mm) thick	< -100
ODS Mo plate	0.25 inch (6.4 mm) thick	< -50

Table 2. Effect of total work and metallurgical condition on creep rupture properties of ODS molybdenum and unalloyed molybdenum.

Material	Product Form	Test Temp (°C)	Stress ksi (MPa)	Metallurgical Condition	Creep Rupture Life (hours)
Mo	Ref. 18	1200	15 (103.4)	RXT	0.25
ODS Mo	0.188 inch (4.8 mm) diameter rod	1200	15 (103.4)	SR	4,100
ODS Mo	0.188 inch (4.8 mm) diameter rod	1200	15 (103.4)	RXT	1,250
Mo	Ref. 18	1500	5 (34.5)	RXT	0.6
ODS Mo	0.188 inch (4.8 mm) diameter rod	1500	5 (34.5)	SR	750
ODS Mo	0.188 inch (4.8 mm) diameter rod	1500	5 (34.5)	RXT	> 2,000
Mo	Ref. 18	1700	5 (34.5)	RXT	0.03
ODS Mo	0.025 inch (0.75 mm) thick sheet	1700	5 (34.5)	SR	217
ODS Mo	0.025 inch (0.75 mm) thick sheet	1700	5 (34.5)	RXT	> 600

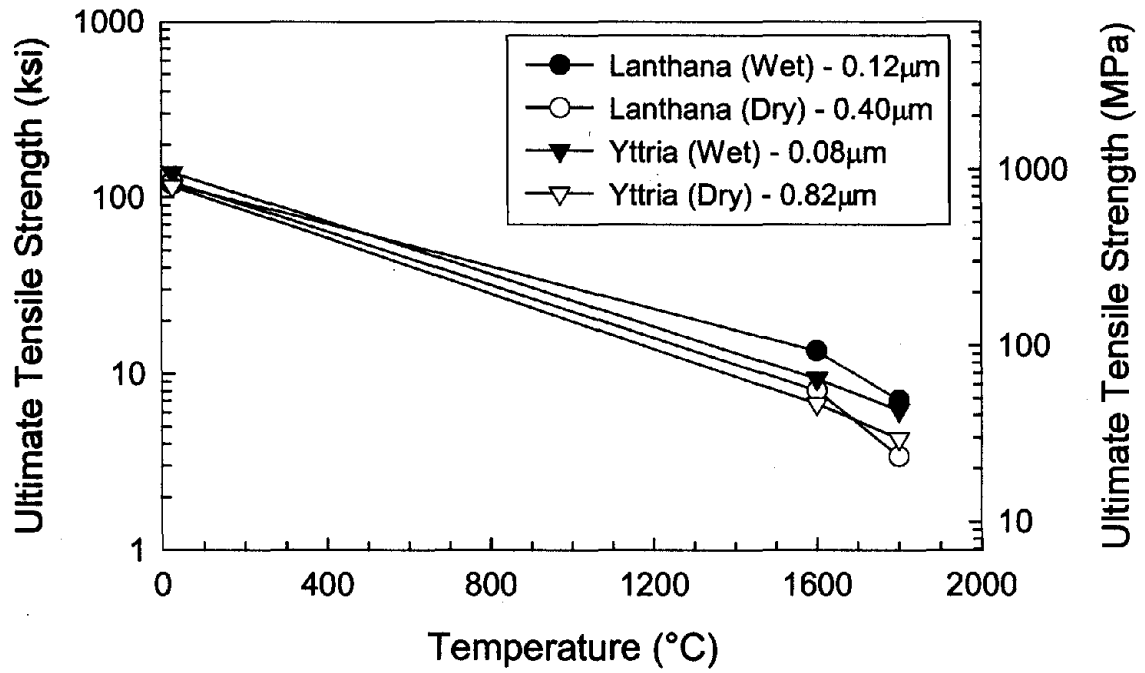


Figure 1. The effect of oxide species and processing method on the strength of 2 vol.% ODS molybdenum material as a function of temperature.

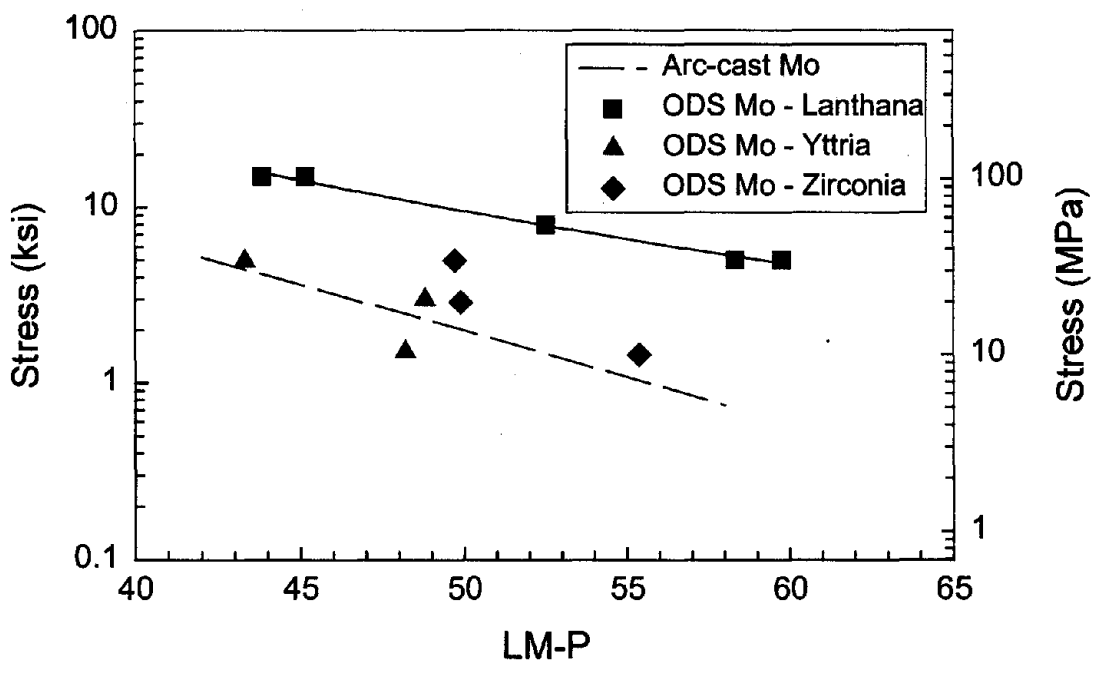


Figure 2. Larson-Miller plot of the stress rupture behavior of various 2 vol.% oxide ODS molybdenum compositions.

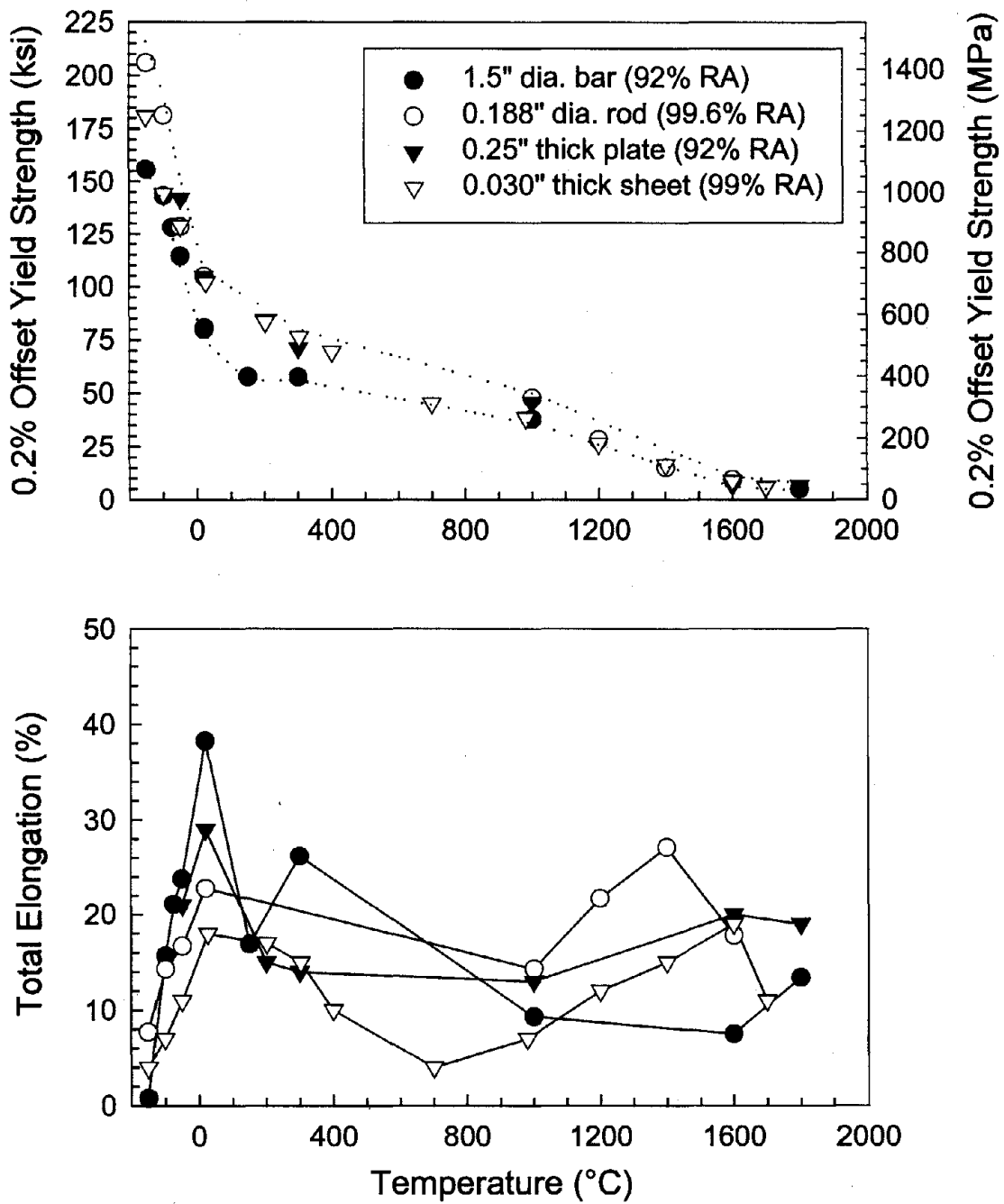


Figure 3. Tensile properties of ODS molybdenum as a function of temperature.

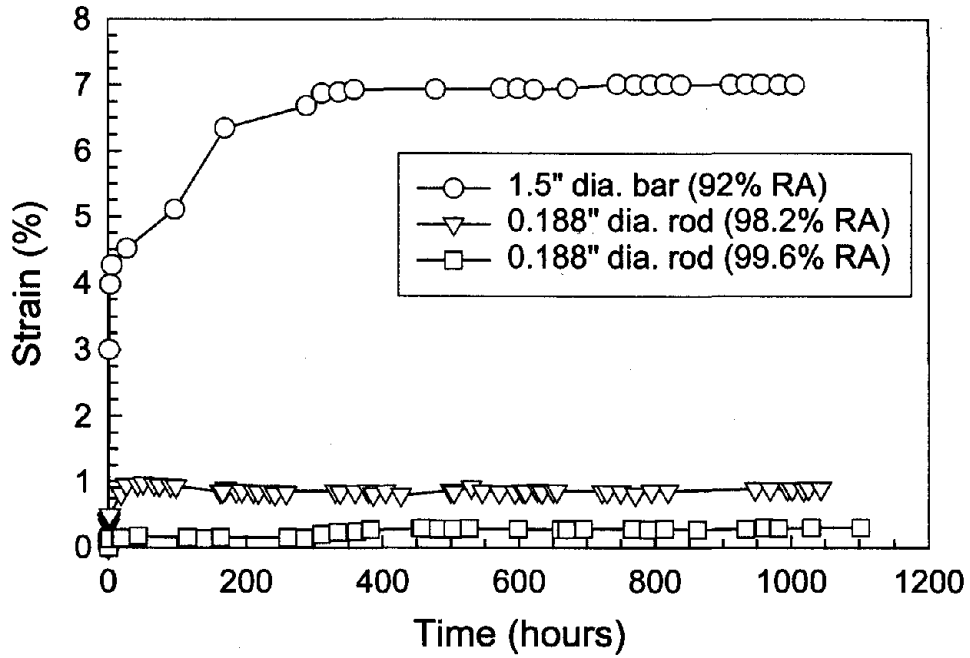


Figure 4. Effect of total cold work on creep resistance of ODS molybdenum; constant load uniaxial creep at 1600°C (2912°F) and 5ksi (34.5MPa).